Published in final edited form as:

J Proteom Genom Res. 2013 ; 1(3): 27–42. doi:10.14302/issn.2326-0793.jpgr-13-257.

Determination of the Proteomic Response to Lapatinib Treatment using a comprehensive and reproducible ion-current-based proteomics strategy

Kathleen O'Connell[*,1], **Jun Li**[2], **Frank Engler**[2], **Kim Hennessy**[3], **Fiona O'Neill**[4], **Robert M. Straubinger**[2], **Jun Qu**[2], and **Robert O'Connor**[4,5]

[1]Department of Chemistry and Biochemistry, University of South Carolina, Columbia, SC

[2]Department of Pharmaceutical Sciences, University at Buffalo, SUNY, Buffalo, NY

[3]National Institute for Cellular Biotechnology, DCU, Glasnevin, Dublin 9

[4]Molecular Therapeutics for Cancer Ireland, National Institute for Cellular Biotechnology, DCU, Glasnevin, Dublin 9

[5]School of Nursing and Human Sciences, DCU, Glasnevin, Dublin 9

Abstract

Lapatinib, a small molecule tyrosine kinase inhibitor is currently used in the treatment of HER2-positive breast cancer. The aim of this study was to further understanding of lapatinib response for the development of novel treatment lapatinib-focussed treatment strategies.

HER2-overexpressing SKBR3 breast cancer cells were treated with lapatinib for 12 hours and the resultant proteome analyzed by a comprehensive ion-current-based LC-MS strategy.

Among the 1224 unique protein identified from SKBR3 cell lysates, 67 showed a significant change in protein abundance in response to lapatinib. Of these, CENPE a centromeric protein with increased abundance, was chosen for further validation. Knockdown and inhibition of CENPE demonstrated that CENPE enhances SKBR3 cell survival in the presence of lapatinib.

Based on this study, CENPE inhibitors may warrant further investigation for use in combination with lapatinib.

Keywords

Breast; Cancer; LC-MS; lapatinib; HER2; CENPE

Corresponding Author: Kathleen O'Connell; Department of Chemistry and Biochemistry, University of South Carolina, 631, Sumter Street, Columbia, SC 29208 USA; Ph:+1 803 777 9381; kathleenoconnell@gmail.com.

Conflicts of interests

The authors declare no conflict of interest.

Introduction

HER2, a member of the Human Epidermal growth factor Receptor (HER) family, is overexpressed in approximately 25% of breast cancers, resulting in the constitutive activation of tyrosine kinase signalling driving tumour cell growth [1]. This plays a crucial role in cancer pathogenesis and is associated with increased tumour invasiveness and poor prognosis [2][3][4].

Lapatinib (GW572016, GlaxoSmithKline Kline, Research Triangle Park, NC), acts as a dual tyrosine kinase inhibitor of EGFR and HER-2 competing with adenosine triphosphate for its binding site on these receptors. This inhibits phosphorylation of EGFR and HER2, with downstream effects on cell survival and proliferation [5]. In 2007, the US FDA approved lapatinib in combination with capecitabine for second line treatment of HER2-positive breast cancer patients [6].

Proteomics has been used to identify different breast cancer subtypes [7][8], and to identify HER2 signalling proteins [9]. Genomic profiles of lapatinib response in breast cancer have been carried out, however, no proteomic studies have been published to date [10] [11]. Characterisation of cellular responses to lapatinib may have significant importance for the identification of markers of lapatinib response and to identify potential drug targets made available by lapatinib treatment thereby improving efficacy. Identification of drug-responsive proteins via proteomics approaches remains highly challenging, due to the wide dynamic range of a typical cellular proteome and the fact that most regulatory proteins are of lower abundance [12][13]. In order to achieve high proteomic coverage and accurate quantification, a comprehensive and reproducible ion-current-based proteomic expression profiling strategy developed in our lab [14][15][16], was employed for the quantification of the response of the SKBR3 cell line to lapatinib.

2 Materials and Methods

2.1 Cell Culture

The breast cancer cell lines SKBR3, BT474, EFM-192a, HCC1954, JIMT-1, UACC-732 and MDA-MB-453 were maintained in RPMI-1640 supplemented with 10% FBS. The SKBR3, BT474, and EFM-192a cell lines are lapatinib sensitive, with IC50 values below 1μM, while JIMT-1, UACC-732 and MDA-MB-453 are lapatinib-insensitive, with IC50 values >1μM [17].

Drug treatments were applied singly or in combinations as follows Laptinib 1μM (Sequoia Sciences, Saint Louis, MO, USA), 150 nM Herceptin (Roche IN, USA), 150 nM Afatinib (Sequoia Sciences) and 20 μM capecitabine (Sigma-Aldrich. St. Loius, MO, USA). Cell pellets were collected pre- and post-drug treatment and lysed in 50 mM Tris, pH 8, 150 mM NaCl, 2% NP-40, 0.5% sodium deoxycholate, and 0.1% SDS. For Western blot, cell lysates were centrifuged at 16,000 *g* for 20 minutes, after 12 hours of drug exposure. For mass spectrometry (MS), the protein lysate was clarified by ultracentrifugation (140,000g, 40 min, 4 °C). Protein concentration was determined by the BCA protein assay kit (Thermo Fischer Scientific, Rockford, IL USA).

IC50 assays were carried out on the SKBR3 cell line with UA62784 (Sigma-Aldrich) at concentrations of 25nM to 300nM and GSK2923295a (Cytokinetics Inc.) at concentrations of 6nM to 300nM. Combination assays were also carried out at these concentrations with 50nM Lapatinib. Drug treatments were carried out 24 hours after cells were seeded ($4*10^4$ cells/96 well) and cell survival measured 5 days later by acid phosphatase assays [18].

2.2 LC-MS/MS

Cell lysates from the SKBR3 cell line (+/− 12 hours 1μM lapatinib, n=6 biological replicates) were tryptically digested using an on-pellet-digestion procedure described previously [15]. A customised nano-LC system [15], was used to separate peptides during a 5-hour LC gradient on a 50 cm 75 μm i.d, C18, 3 μm, 100A column. Mobile phase A was 0.1% formic acid in 2% acetonitrile and mobile phase B was 0.1% formic acid in 84% acetonitrile. The flow rate was 250 nL/min and the gradient profile was (i) a linear increase from 3% to 10% B over 5 min; (ii) an increase from 10 to 24% B over 115 min; (iii) an increase from 24 to 38% B over 70 min; (iv) an increase from 38 to 60% B over 50 min; (v) an increase from 60 to 97% B in 35 min, and finally (vi) isocratic at 97% B for 25 min. The optimal loading amount of peptide was identified experimentally and a loading mass of 6 μg per injection was employed per sample.

LTQ/Orbitrap data was acquired over a period of 275 minutes, one scan cycle included an MS1 scan (m/z 300–2000) at a resolution of 60 000 followed by seven MS2 scans by LTQ, to fragment the seven most abundant precursors. The target value for MS1 by Orbitrap was 4×10^6. The fragmentation type was CID with a normalized collision energy of 35%.

2.3 Relative quantification of Protein changes via ion-current-based strategies

Sieve (Fiona build, v. 1.2, Thermo Scientific), was used for quantitative data analysis. All peptides differing significantly between the control and treated (Fisher's combined probability test, p-value < 0.05) were selected for protein identification. Relative abundance of an individual protein was calculated as the mean AUC ratio for all peptides derived from that protein. Protein ratios were defined as the average abundance of a protein in lapatinib treated samples/control samples. This number was divided into 1 to be converted into +/− fold changes. Identifications were matched against a non-redundant human database derived from the Swissprot database (Feb 2010). The precursor mass tolerance was set to 25 ppm and a mass tolerance of 1.0 Da; fixed modification was carbamidomethyl and variable modifications methionine oxidation. Requirements for a successful identification was matching of at least 2 unique peptides, a peptide probability of >95%, a protein probability of >99% and Sequest restrictions of deltaCn scores of greater than 0.10 and XCorr scores that achieves a 0.5% peptide FDR were employed.

2.4 Analysis of Protein localisation and cellular processes

Raw LC/MS data was also analysed using Scaffold 3 software (Portland, OR) with protein identifications carried out through the Sequest server, as described above. GO annotations were retrieved from a human non-redundant Uniprot database and protein cellular localisation and cell processes represented as a percentage of the overall GO annotations retrieved.

2.5 Western blotting

Equal quantities of protein lysates pre- and post-drug treatment (n=3 biological replicates) were subjected to Western blotting [19]. Antibody binding was visualised by incubating the blot for 5 minutes with ECL Plus Western Blotting Detection substrate (RPN2132, GE Healthcare, PA, USA) and florescence emission captured by scanning blots at 457 nm excitation, 520 nm emission (PMT 450) on a Typhoon Variable Trio 9400 scanner. Antibodies for TET2 (S-13, sc-136926), HER2 ([3B5], ab16901), CENPE (C-7488) and b-actin (A3854) were purchased from Santa Cruz Biotechnologies (CA, USA), Abcam (Cambridge, UK) and Sigma-Aldrich respectively.

2.6 qRT-PCR

qRT-PCR was carried out as previously described [10]. RNA was isolated with Rneasy Mini kit (Qiagen, CA, USA, n=3 biological replicates). Primers, buffer and dNTPs were supplied by a High Capacity cDNA Reverse Transcription kit (Applied Biosystems). CENPE specific FAM-labelled primer (Hs0106824_m1, Applied Biosystems) was used to quantify CENPE cDNA by qPCR; GAPDH specific FAM label primer (Hs9999905_m1) was used to measure GAPDH cDNA, which acted as an endogenous control.

2.7 siRNA

3×10^4 SKBR3 cells/well were transfected over 24 hours, in a 24 well plate, using 1 μl siPORT Neofx transfection reagent (Applied Biosystems). siRNA knockdown was performed using 30nM scrambled control (Negative Control #2, Applied Biosystems), and 30nM CENPE siRNA (S2917, Applied Biosystems). Neofx was incubated with serum free Optimem media for 10 minutes, mixed with diluted siRNA, and incubated for another 10 mins. The Neofx-siRNA mix was then applied to cells. Post-24 hours fresh media +/− 100nM lapatinib was added to transfected cells; drug treatments lasted 5 days. Cells were then trypsinised and incubated with 1 part cell suspension: 3 parts Guava viacount reagent and incubated in the dark for 5 minutes before viable cells were counted on a Guava Easycyte (EMD Millipore, MA, USA).

3 Results

3.1 Label-free profiling of the response to lapatinib

A comprehensive, in-depth proteomic investigation is essential for a study of this nature. As the whole cell lysate is highly complex, a large number of tryptic peptides are retrieved by the on-pellet digestion procedure. To achieve sufficient chromatographic separation, high run-to-run reproducibility of retention times we employed a custom nano-LC/nanospray configuration.

In total, 1224 unique proteins were identified with high confidence and subsequently quantified. The full list of the proteins analyzed in this study, as well as the information on the peptides identified, is shown in SI Table 1. Among the 1224 protein analyzed, quantitative proteomic profiling of the SKBR3 cell line revealed an altered abundance of 67 proteins in lapatinib-treated compared to untreated cells. Of these, 21 demonstrated an increased abundance and 46 a decreased abundance in the treated cells. The cut-off for

biomarker discovery was based on the calculation of the false-positive biomarker discovery rate, as described in our previous publications [14][15]. Listed in Table 1, divided by function, are the protein names, number of peptides, p-values, and fold change of these proteins.

A Gene Ontology (GO) analysis of the identified proteins was performed using DAVID Bioinformatics Resources 6.7 (http://david.abcc.ncifcrf.gov/). A large number of proteins from plasma membrane and various organelles were identified indicating a comprehensive protein recovery by our gel-free sample preparation procedure 1A).

HER2 and TET2 were chosen for validation of LC-MS/MS data by Western blot. Both proteins were assessed in 7 cell lines (4 sensitive to lapatinib, 3 insensitive), Figure 1B. While TET2 was significantly changed in all 4 lapatinib sensitive cell lines, and not in the insensitive, HER2 only showed a significant increase in the SKBR3 cell line ($p<0.05$).

3.2 Validation of increased CENPE protein

CENPE, a protein with increased abundance (2.3 fold) in lapatinib-treated cells was also chosen for validation as it represented a possible target for therapeutic intervention as a specific drug-based inhibitor was available. Changes to CENPE abundance were assessed by Western blot (Figure 2A) with significant increases found in 4 lapatinib-sensitive cell lines ($p<0.05$). Additionally, qRT-PCR analysis, carried out to assess if any related changes were occurring in mRNA expression (Figure 2B), showed significant increases in CENPE mRNA in 4 lapatinib-sensitive cell lines (Figure 2B).

3.3 Alterations in CENPE in response to other HER2 targeted agents

To determine if this trend of increased CENPE abundance was purely a lapatinib drug response, or if CENPE could alter the toxicological response to lapatinib in a clinically-relevant manner, CENPE protein levels were tested in response to a) other HER2 targeting agents and b) clinically relevant combinations of lapatinib with other drugs. In the SKBR3 and BT474 cell lines both afatinib (irreversible HER2 and EGFR inhibitory small molecule agent) and trastuzumab (HER2-inhibitory monoclonal antibody) treatment alone resulted in significantly decreased CENPE protein abundance, in contrast to lapatinib alone treatment (Figure 3).

In contrast to the decreases shown when cells were treated by trastuzumab alone, the combination of lapatinib and trastuzumab resulted in 2–3 fold increases in CENPE protein in both the SKBR3 and BT474 cell lines (Figure 3). The combination of lapatinib and capecitabine also resulted in a similar increase in CENPE protein in both cell lines (Figure 3).

3.4 CENPE inhibition in combination with lapatinib

To evaluate if the combination of lapatinib and CENPE inhibition resulted in decreased cell growth, compared to either lapatinib alone or CENPE inhibition alone, siRNA knockdown of CENPE was carried out.

Knockdown of CENPE in SKBR3 cells resulted in approximately a 70% decrease in CENPE protein after 5 days (Figure 4A). This treatment had very little effect on cell survival (<1%). Lapatinib-treated cells showed a 63% decrease in cell survival. The combination of lapatinib and CENPE knockdown resulted in a even greater decrease in cell survival of 85% (Figure 4A).

To determine if small molecule inhibitors would demonstrate a similar effect as siRNA, UA62784, a laboratory grade inhibitor of CENPE, was tested alone in the nM range (0–300nM) and in combination with 50nM lapatinib. The IC50 value of UA62784 in the SKBR3 cell line was 144nM, comparable but slightly higher than those published for other cancer cell lines [20]. At the lower nM ranges of UA63784, the addition of lapatinib resulted in significant decreases in cell survival compared to lapatinib or UA63784 alone (Figure 4B); the IC50 value of UA63784 when in combination with lapatinib dropped to 15nM.

The IC50 for another CENPE inhibitor, GSK23295A alone was lower at 16nM, than for UA62784 alone. Combination of this agent with 50 nM lapatinib resulted in an IC50 of 5nM for GSK23295A. Again at the lower end of the treatment range the combination of lapatinib and GSK23295A displayed synergy (Figure 4C).

4 Discussion

In order to further understand how lapatinib treatment affects HER2 positive cells we studied lapatinib-sensitive SKBR3 cells, in the absence and presence of lapatinib, by LC-MS using a highly optimised and reproducible ion-current strategy [15].

This approach resulted in the identification of 67 proteins that had altered abundance in response to lapatinib treatment. Western blotting analysis of two proteins, HER2 and TET2, confirmed the accuracy of MS results for the SKBR3 and highlighted the importance of validating results in multiple cells lines. CENPE, a mitotic checkpoint protein, acts as a kinesin-like motor protein aiding in the segregation of chromosomes and plays a role in the mitotic checkpoint by binding to and regulating activation of BUBR1 [21, 22]. CENPE is present in normal cells at low levels during G1 and accumulates during late G2 and M-phases [23]. It is over expressed in invasive breast tumours compared to normal breast tissue [24]. There is no known association of CENPE with HER2 nor with lapatinib response. In this study, CENPE demonstrated increased protein and mRNA abundance in lapatinib sensitive breast cancer cells after treatment with Lapatinib. This CENPE response seems to be specific to lapatinib as other HER2 targeting drugs, namely afatinib and trastuzumab, did not result in increased CENPE expression. Lapatinib is currently administered with capecitabine [6] and is undergoing testing in combination with trastuzumab [25], the combination of either drug with lapatinib resulted in increased CENPE protein. This suggests that lapatinib, even when administered with additional anticancer agents, will result in increased CENPE expression.

Previous studies have shown that it is possible to target alterations that occur in a cell in response to a drug, further sensitising the treated cells to that drug [26] [27]. As kinesins and

kinesin-like proteins represent promising molecular targets in cancer it was decided to investigate the effect of CENPE inhibition on lapatinib-treated SKBR3 cells [28].

Reduction of CENPE expression has been implicated in tumour formation, however, it seems to have contradictory roles, both promoting tumourogensis at low levels of genomic instability (specifically ploidy) and inhibiting tumourogensis when a higher threshold is reached [29]. siRNA knockdown of CENPE results in arrest at the G2/M phase of the cell cycle [30]. CENPE inhibition by siRNA had a greater effect on lapatinib-treated cells than lapatinib alone. As small molecule inhibitors and monoclonal antibodies remain the current platform for targeted therapies, and may represent more efficient inhibition of target activity than siRNA, two small molecule drugs, UA62784 [20] and GSK923295A [31] were applied to SKBR3 cells alone and in combination with lapatinib. Initial publication of UA62784 data suggest that it is a specific inhibitor of CENPE but this has subsequently been challenged [32]; no such controversy exists with regards to GSK923295A. Both UA62784 and GSK923295A demonstrated synergy in combination with lapatinib. The data suggests CENPE inhibition in combination with lapatinib may, with further investigation, be a novel treatment strategy. Should UA62784 ultimately prove to be a microtubule inhibitor, as suggested, lapatinib may sensitise HER2 positive breast cancer cells to a wider range of microtubule and mitotic checkpoint protein inhibitors.

Acknowledgments

The authors wish to thank the Science Foundation Ireland, Strategic Research Cluster award to Molecular Therapeutics for Cancer Ireland (award 08/SRC/B1410) for funding this work.

References

1. Slamon DJ, Leyland-Jones B, Shak S, Fuchs H, Paton V, Bajamonde A, et al. Use of chemotherapy plus a monoclonal antibody against HER2 for metastatic breast cancer that overexpresses *HER2*. N Engl J Med. 2001 Mar 15; 344(11):783–92. [PubMed: 11248153]
2. Hudziak RM, Schlessinger J, Ullrich A. Increased expression of the putative growth factor receptor p185HER2 causes transformation and tumorigenesis of NIH 3T3 cells. Proc Natl Acad Sci U S A. 1987 Oct; 84(20):7159–63. [PubMed: 2890160]
3. Woods Ignatoski KM, Grewal NK, Markwart S, Livant DL, Ethier SP. p38MAPK induces cell surface alpha4 integrin downregulation to facilitate erbB-2-mediated invasion. Neoplasia. 2003 Mar-Apr;5(2):128–34. [PubMed: 12659685]
4. Toikkanen S, Helin H, Isola J, Joensuu H. Prognostic significance of HER-2 oncoprotein expression in breast cancer: a 30-year follow-up. J Clin Oncol. 1992 Jul; 10(7):1044–8. [PubMed: 1351537]
5. Rusnak DW, Affleck K, Cockerill SG, Stubberfield C, Harris R, Page M, et al. The characterization of novel, dual ErbB-2/EGFR, tyrosine kinase inhibitors: potential therapy for cancer. Cancer Res. 2001 Oct 1; 61(19):7196–203. [PubMed: 11585755]
6. Ryan Q, Ibrahim A, Cohen MH, Johnson J, Ko CW, Sridhara R, et al. FDA drug approval summary: lapatinib in combination with capecitabine for previously treated metastatic breast cancer that overexpresses HER-2. Oncologist. 2008 Oct; 13(10):1114–9. [PubMed: 18849320]
7. Chen H, Pimienta G, Gu Y, Sun X, Hu J, Kim MS, et al. Proteomic characterization of Her2/neu-overexpressing breast cancer cells. Proteomics. Nov; 10(21):3800–10.
8. Lu M, Whelan SA, He J, Saxton RE, Faull KF, Whitelegge JP, et al. Hydrophobic Proteome Analysis of Triple Negative and Hormone-Receptor-Positive-Her2-Negative Breast Cancer by Mass Spectrometer. Clin Proteomics. Sep; 6(3):93–103. [PubMed: 20930921]

9. Bose R, Molina H, Patterson AS, Bitok JK, Periaswamy B, Bader JS, et al. Phosphoproteomic analysis of Her2/neu signaling and inhibition. Proc Natl Acad Sci U S A. 2006 Jun 27; 103(26): 9773–8. [PubMed: 16785428]
10. O'Neill F, Madden SF, Aherne ST, Clynes M, Crown J, Doolan P, et al. Gene expression changes as markers of early lapatinib response in a panel of breast cancer cell lines. Mol Cancer. Jun 18.11(1):41.
11. Hegde PS, Rusnak D, Bertiaux M, Alligood K, Strum J, Gagnon R, et al. Delineation of molecular mechanisms of sensitivity to lapatinib in breast cancer cell lines using global gene expression profiles. Mol Cancer Ther. 2007 May; 6(5):1629–40. [PubMed: 17513611]
12. Qu J, Jusko WJ, Straubinger RM. Utility of cleavable isotope-coded affinity-tagged reagents for quantification of low-copy proteins induced by methylprednisolone using liquid chromatography/tandem mass spectrometry. Anal Chem. 2006 Jul 1; 78(13):4543–52. [PubMed: 16808464]
13. Anderson DC, Campbell EL, Meeks JC. A soluble 3D LC/MS/MS proteome of the filamentous cyanobacterium Nostoc punctiforme. J Proteome Res. 2006 Nov; 5(11):3096–104. [PubMed: 17081061]
14. Qu J, Lesse AJ, Brauer AL, Cao J, Gill SR, Murphy TF. Proteomic expression profiling of Haemophilus influenzae grown in pooled human sputum from adults with chronic obstructive pulmonary disease reveal antioxidant and stress responses. BMC Microbiol. 2010; 10:162. [PubMed: 20515494]
15. Duan X, Young R, Straubinger RM, Page B, Cao J, Wang H, et al. A straightforward and highly efficient precipitation/on-pellet digestion procedure coupled with a long gradient nano-LC separation and Orbitrap mass spectrometry for label-free expression profiling of the swine heart mitochondrial proteome. J Proteome Res. 2009 Jun; 8(6):2838–50. [PubMed: 19290621]
16. Vagin VV, Wohlschlegel J, Qu J, Jonsson Z, Huang X, Chuma S, et al. Proteomic analysis of murine Piwi proteins reveals a role for arginine methylation in specifying interaction with Tudor family members. Genes Dev. 2009 Aug 1; 23(15):1749–62. [PubMed: 19584108]
17. O'Brien NA, Browne BC, Chow L, Wang Y, Ginther C, Arboleda J, et al. Activated phosphoinositide 3-kinase/AKT signaling confers resistance to trastuzumab but not lapatinib. Mol Cancer Ther. Jun; 9(6):1489–502.
18. Martin A, Clynes M. Acid phosphatase: endpoint for in vitro toxicity tests. In Vitro Cell Dev Biol. 1991 Mar; 27A(3 Pt 1):183–4. [PubMed: 2033016]
19. O'Connell K, Prencipe M, O'Neill A, Corcoran C, Rani S, Henry M, et al. The use of LC-MS to identify differentially expressed proteins in docetaxel-resistant prostate cancer cell lines. Proteomics. Jul; 12(13):2115–26.
20. Henderson MC, Shaw YJ, Wang H, Han H, Hurley LH, Flynn G, et al. UA62784, a novel inhibitor of centromere protein E kinesin-like protein. Mol Cancer Ther. 2009 Jan; 8(1):36–44. [PubMed: 19139111]
21. Mao Y, Abrieu A, Cleveland DW. Activating and silencing the mitotic checkpoint through CENP-E-dependent activation/inactivation of BubR1. Cell. 2003 Jul 11; 114(1):87–98. [PubMed: 12859900]
22. Abrieu A, Kahana JA, Wood KW, Cleveland DW. CENP-E as an essential component of the mitotic checkpoint in vitro. Cell. 2000 Sep 15; 102(6):817–26. [PubMed: 11030625]
23. Brown KD, Coulson RM, Yen TJ, Cleveland DW. Cyclin-like accumulation and loss of the putative kinetochore motor CENP-E results from coupling continuous synthesis with specific degradation at the end of mitosis. J Cell Biol. 1994 Jun; 125(6):1303–12. [PubMed: 8207059]
24. Bieche I, Vacher S, Lallemand F, Tozlu-Kara S, Bennani H, Beuzelin M, et al. Expression analysis of mitotic spindle checkpoint genes in breast carcinoma: role of NDC80/HEC1 in early breast tumorigenicity, and a two-gene signature for aneuploidy. Mol Cancer. 10:23.
25. Baselga J, Bradbury I, Eidtmann H, Di Cosimo S, de Azambuja E, Aura C, et al. Lapatinib with trastuzumab for HER2-positive early breast cancer (NeoALTTO): a randomised, open-label, multicentre, phase 3 trial. Lancet. Feb 18; 379(9816):633–40.
26. Astsaturov I, Ratushny V, Sukhanova A, Einarson MB, Bagnyukova T, Zhou Y, et al. Synthetic lethal screen of an EGFR-centered network to improve targeted therapies. Sci Signal. 3(140):ra67. [PubMed: 20858866]

27. Azorsa DO, Gonzales IM, Basu GD, Choudhary A, Arora S, Bisanz KM, et al. Synthetic lethal RNAi screening identifies sensitizing targets for gemcitabine therapy in pancreatic cancer. J Transl Med. 2009; 7:43. [PubMed: 19519883]

28. Huszar D, Theoclitou ME, Skolnik J, Herbst R. Kinesin motor proteins as targets for cancer therapy. Cancer Metastasis Rev. 2009 Jun; 28(1–2):197–208. [PubMed: 19156502]

29. Weaver BA, Silk AD, Montagna C, Verdier-Pinard P, Cleveland DW. Aneuploidy acts both oncogenically and as a tumor suppressor. Cancer Cell. 2007 Jan; 11(1):25–36. [PubMed: 17189716]

30. Tanudji M, Shoemaker J, L'Italien L, Russell L, Chin G, Schebye XM. Gene silencing of CENP-E by small interfering RNA in HeLa cells leads to missegregation of chromosomes after a mitotic delay. Mol Biol Cell. 2004 Aug; 15(8):3771–81. [PubMed: 15181147]

31. Lock RB, Carol H, Morton CL, Keir ST, Reynolds CP, Kang MH, et al. Initial testing of the CENP-E inhibitor GSK923295A by the pediatric preclinical testing program. Pediatr Blood Cancer. Jun; 58(6):916–23.

32. Tcherniuk S, Deshayes S, Sarli V, Divita G, Abrieu A. UA62784 Is a cytotoxic inhibitor of microtubules, not CENP-E. Chem Biol. May 27; 18(5):631–41.

A

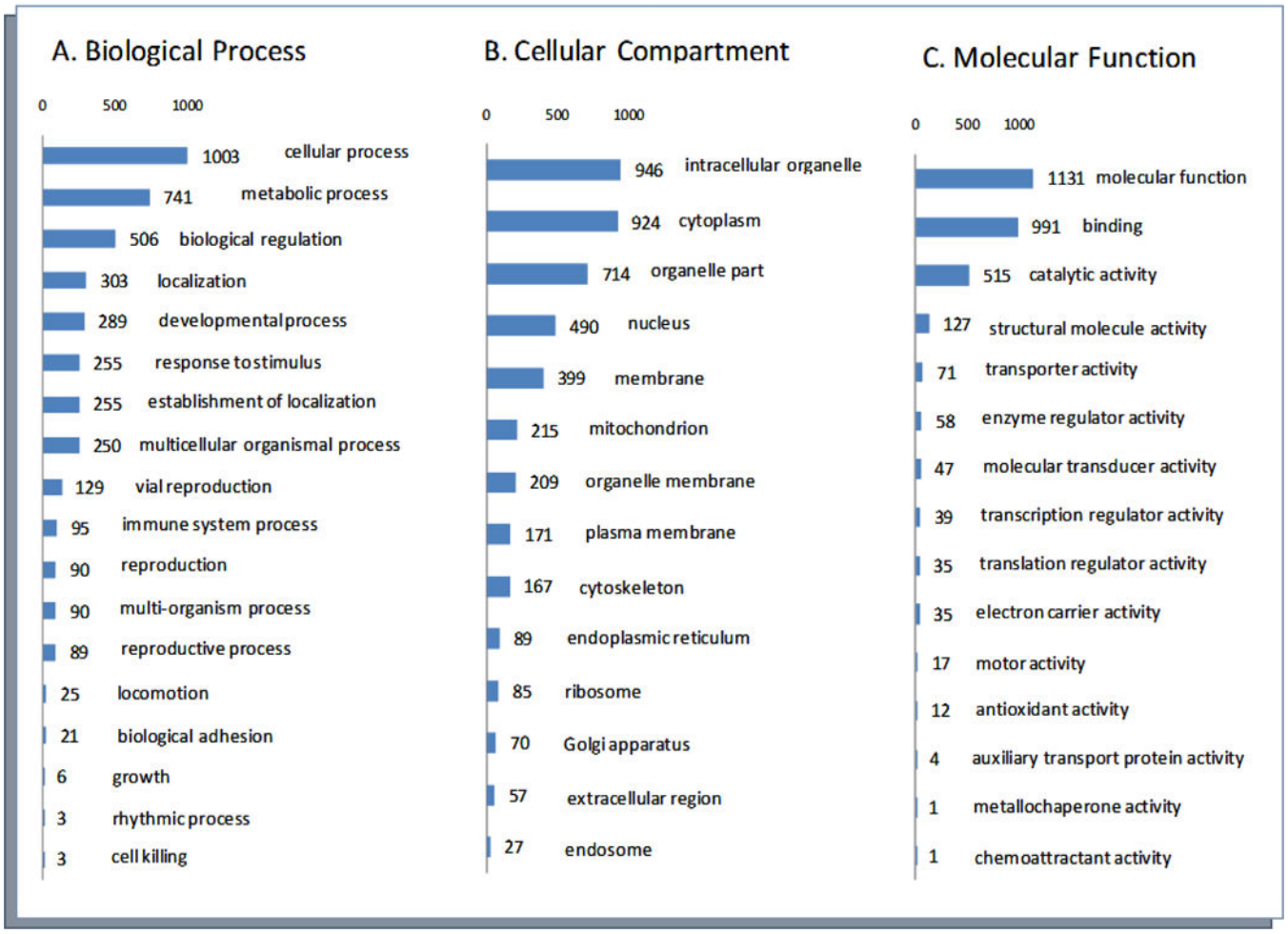

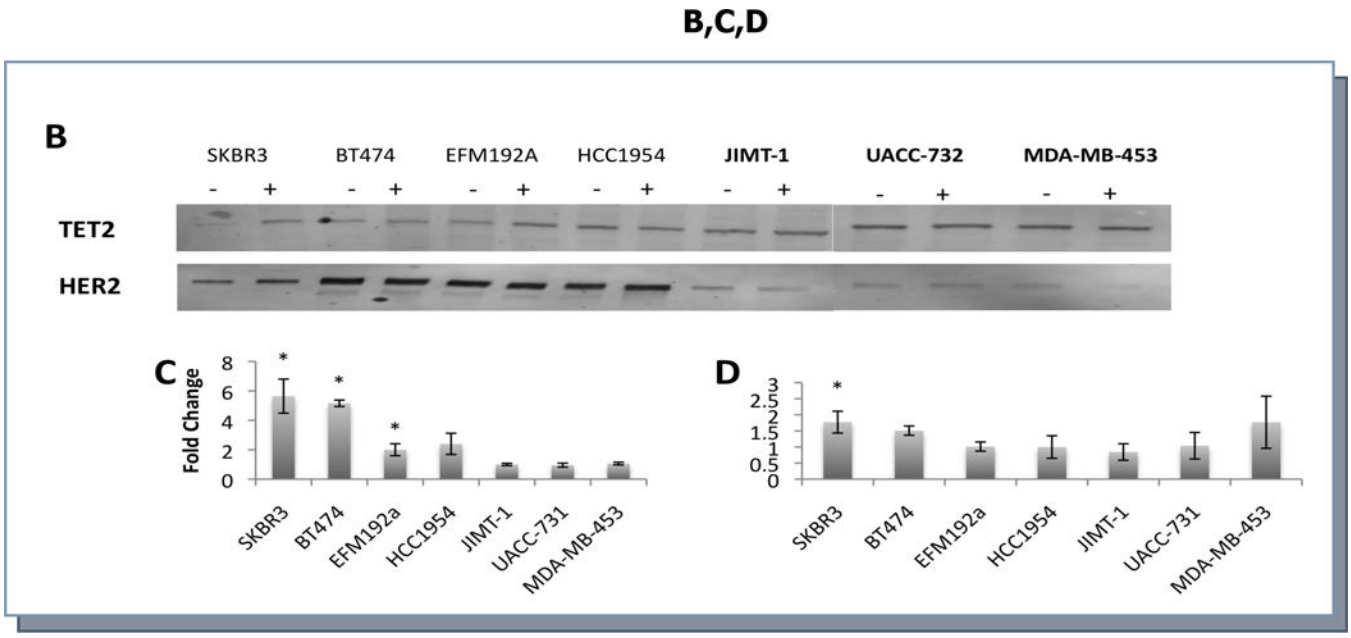

Figure 1.

A) Classifications of the 1224 unique proteins by Biological process, Cellular Compartment and Molecular function

B) TET2 and HER2 expression, in the absence (−) or presence (+) of 1μM lapatinib after 12 hours, in lapatinib sensitive cell lines and lapatinib insensitive cell lines (highlighted in bold)

C) TET2 and **D)** HER2 densitometry. Fold change = Control vs. Lapatinib treated. * represents significance at $p<0.05$ by Students *t*-test

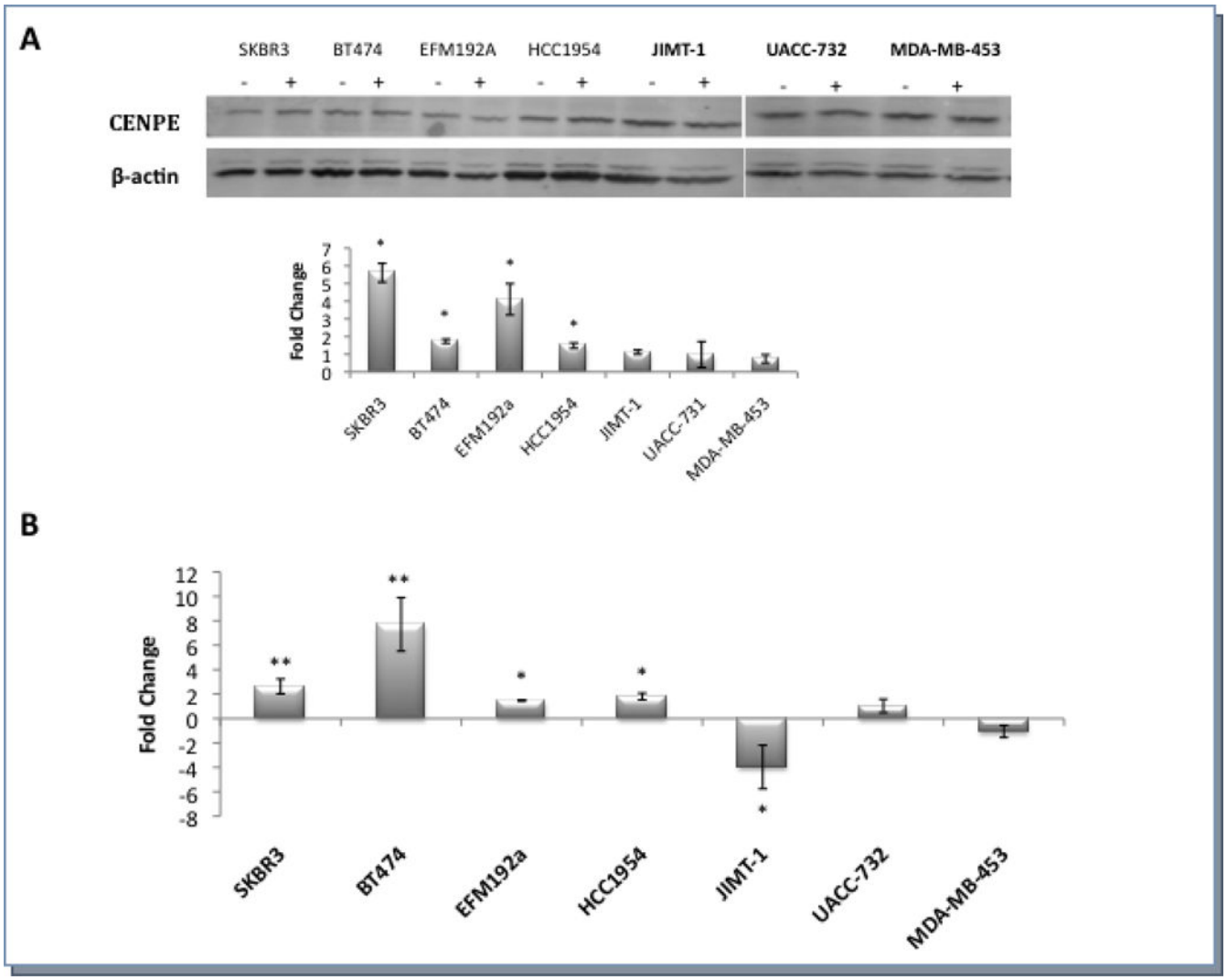

Figure 2.

Expression of CENPE, in the absence (−) or presence (+) of 1μM lapatinib after 12 hours, in lapatinib sensitive cell lines and lapatinib insensitive cell lines (highlighted in bold)

A) By western blot including densitometric measurement of protein fold change (control vs. Lapatinib treated).

B) qRT-PCR measurement of expression changes of mRNA (control vs. Lapatinib treated)

* represents significance at $p<0.05$ ** at $p<0.01$ by Students *t*-test

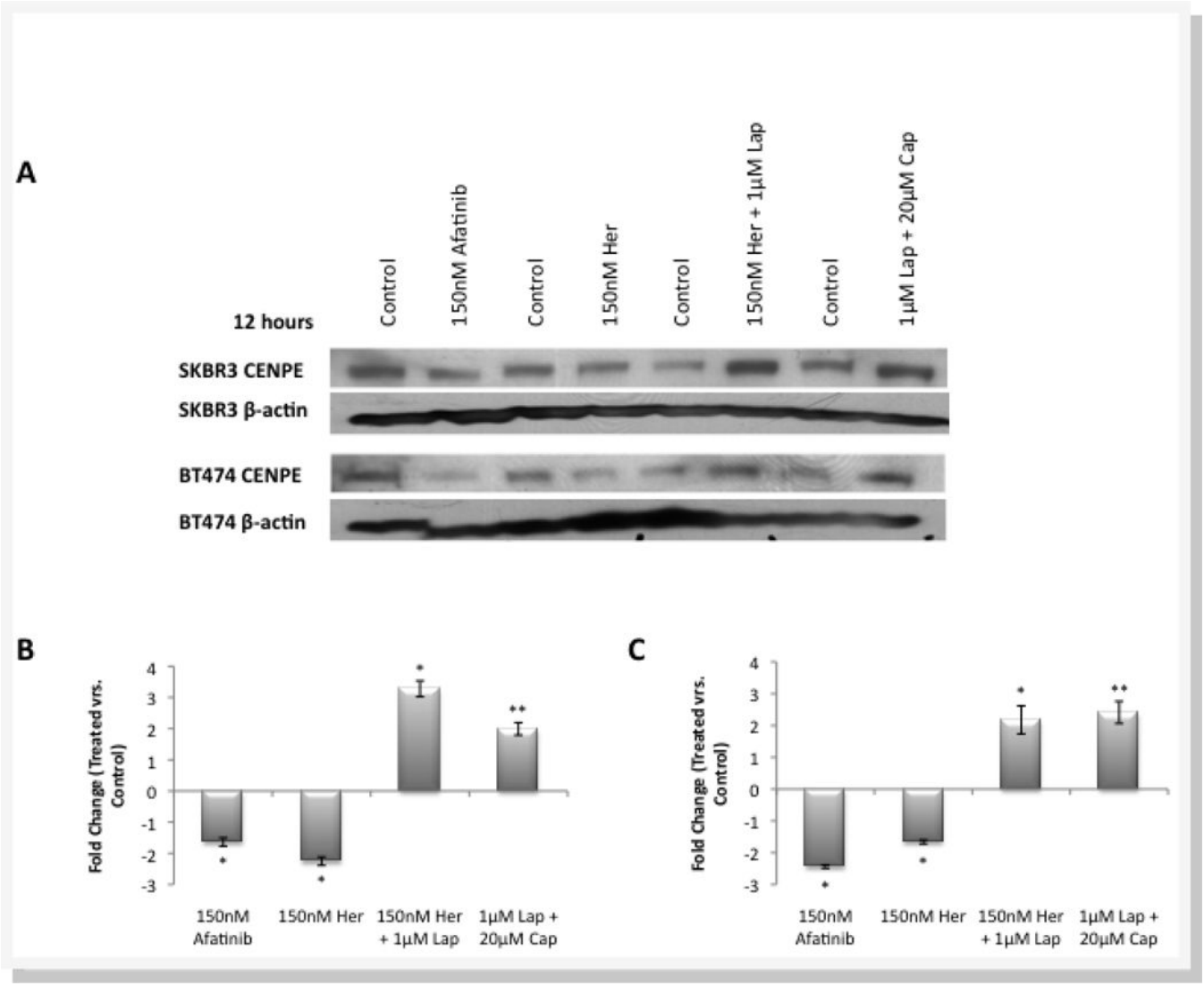

Figure 3.

A) CENPE protein expression in response to a 12 hour treatment with 150nM Afatinib, 150nM Trastuzumab (Her), 150nM Trastuzumab + 1μM Lapatinib (Lap) and 1μM Lapatinib + 20μM Capecitabine (Cap) with densitometric measurement of fold change (control vs. drug treated) in B) the SKBR3 cell line and C) the BT474 cell line. * represents significance at $p<0.05$ ** at $p<0.01$ by Students *t*-test

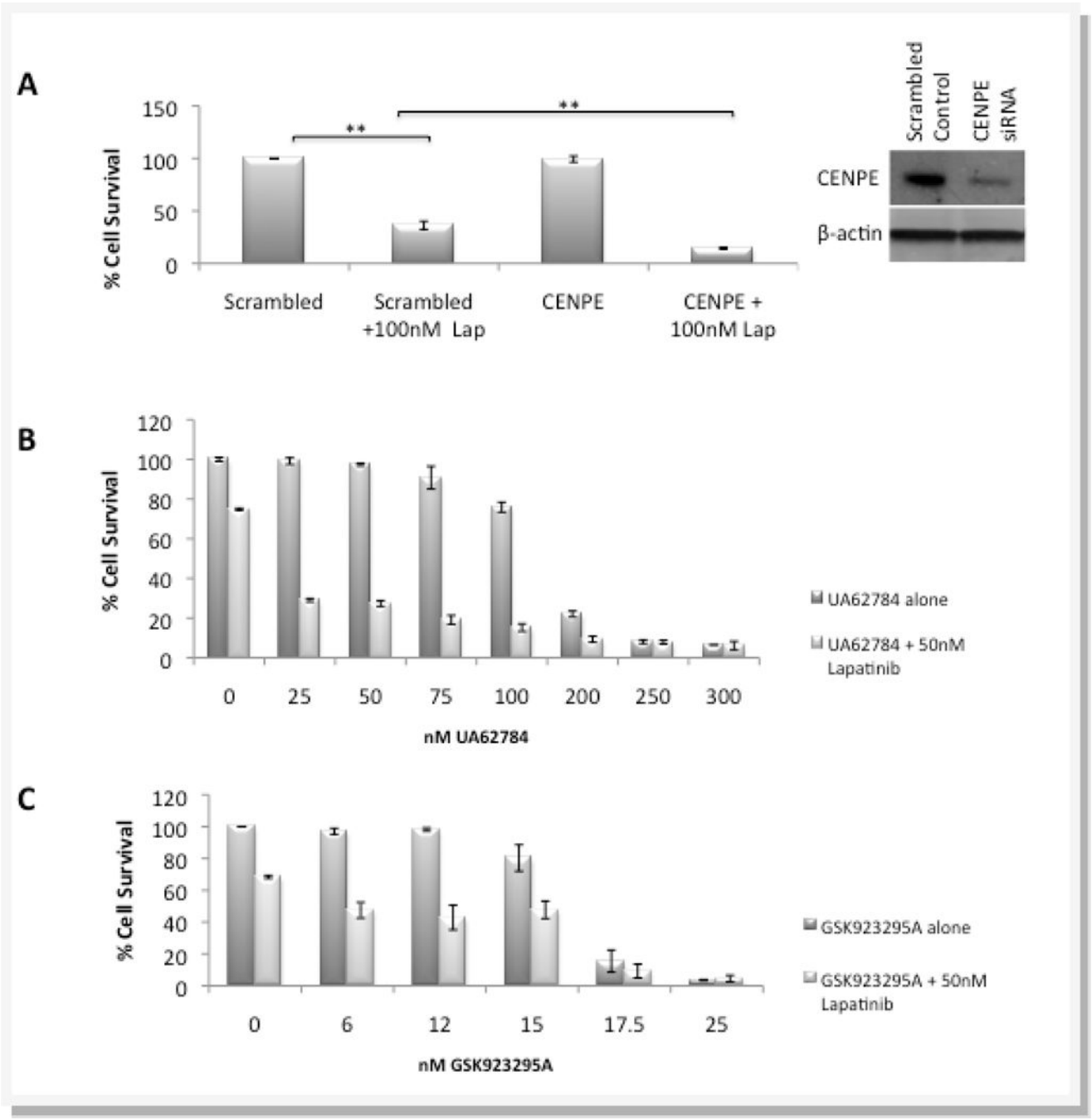

Figure 4.

A) The effect of CENPE knockdown by siRNA, with and without 100nM Lapatinib, on cell viability. Knockdown of CENPE expression confirmed by western blot.

B) Effect on cell viability (after 5 days) by the CENPE inhibitor UA62784, alone and in combination with 50nM Lapatinib.

C) Effect on cell viability (after 5 days) by the CENPE inhibitor GSK923295A, alone and in combination with 50nM Lapatinib. * represents significance at $p<0.05$ ** at $p<0.01$ by Students *t*-test

Table 1

List of proteins identified to have altered protein abundance in response to lapatinib, grouped according to biological function

Uniprot I.D	Protein	No of Unique Peptides	p-value	Fold Change
Metabolic				
Q15111	PLCL1 Inactive phospholipase C-like protein 1	2	1.60E-02	1.47
O95861	BPNT1 3_(2_),5_-bisphosphate nucleotidase 1	2	2.30E-02	1.37
P30038	AL4A1 Delta-1-pyrroline-5-carboxylate dehydrogenase, mitochondrial	3	1.70E-03	−1.36
P07205	PGK2 Phosphoglycerate kinase 2	4	4.90E-02	−1.39
Q9Y6M9	NDUB9 NADH dehydrogenase [ubiquinone] 1 beta subcomplex subunit 9	2	4.70E-02	−1.41
P49327	FAS Fatty acid synthase	48	1.00E-05	−1.44
P06733	ENOA Alpha-enolase	12	1.90E-02	−2.7
Cytoskeletal				
Q8IWC1	MA7D3 MAP7 domain-containing protein 3	2	1.10E-02	1.61
Q96JE9	MAP6 Microtubule-associated protein 6	2	4.90E-03	1.5
P09493	TPM1 Tropomyosin alpha-1 chain	9	4.70E-03	−1.35
P17661	DESM Desmin	3	9.90E-20	−1.41
P02538	K2C6A Keratin, type II cytoskeletal 6A	5	8.40E-06	−1.35
P48668	K2C6C Keratin, type II cytoskeletal 6C	4	1.50E-06	−1.35
P04259	K2C6B Keratin, type II cytoskeletal 6B	4	1.50E-06	−1.35
P41219	PERI Peripherin	2	9.90E-20	−1.39
Q27J81	INF2 Inverted formin-2	2	9.60E-03	−1.63
Metabolic				
Q15111	PLCL1 Inactive phospholipase C-like protein 1	2	1.60E-02	1.47
O95861	BPNT1 3_(2_),5_-bisphosphate nucleotidase 1	2	2.30E-02	1.37
P30038	AL4A1 Delta-1-pyrroline-5-carboxylate dehydrogenase, mitochondrial	3	1.70E-03	−1.36
P07205	PGK2 Phosphoglycerate kinase 2	4	4.90E-02	−1.39
Q9Y6M9	NDUB9 NADH dehydrogenase [ubiquinone] 1 beta subcomplex subunit 9	2	4.70E-02	−1.41
P49327	FAS Fatty acid synthase	48	1.00E-05	−1.44
P06733	ENOA Alpha-enolase	12	1.90E-02	−2.7
Cytoskeletal				
Q8IWC1	MA7D3 MAP7 domain-containing protein 3	2	1.10E-02	1.61
Q96JE9	MAP6 Microtubule-associated protein 6	2	4.90E-03	1.5
P09493	TPM1 Tropomyosin alpha-1 chain	9	4.70E-03	−1.35
P17661	DESM Desmin	3	9.90E-20	−1.41
P02538	K2C6A Keratin, type II cytoskeletal 6A	5	8.40E-06	−1.35
P48668	K2C6C Keratin, type II cytoskeletal 6C	4	1.50E-06	−1.35

Uniprot I.D	Protein	No of Unique Peptides	p-value	Fold Change
P04259	K2C6B Keratin, type II cytoskeletal 6B	4	1.50E-06	−1.35
P41219	PERI Peripherin	2	9.90E-20	−1.39
Q27J81	INF2 Inverted formin-2	2	9.60E-03	−1.63
Chromatin				
P0C0S8	H2A1 Histone H2A type 1	4	2.20E-16	−2.05
P20671	H2A1D Histone H2A type 1-D	4	2.20E-16	−2.05
Q16777	H2A2C Histone H2A type 2-C	4	2.20E-16	−2.05
Q6FI13	H2A2A Histone H2A type 2-A	4	2.20E-16	−2.05
Q96KK5	H2A1H Histone H2A type 1-H	4	2.20E-16	−2.05
Q99878	H2A1J Histone H2A type 1-J	4	2.20E-16	−2.05
Q9BTM1	H2AJ Histone H2A.J	4	2.20E-16	−2.05
P68431	H31 Histone H3.1	4	1.50E-04	−2.11
P84243	H33 Histone H3.3	4	1.50E-04	−2.11
Q16695	H31T Histone H3.1t	4	1.50E-04	−2.11
Q71DI3	H32 Histone H3.2	4	1.50E-04	−2.11
P10412	H14 Histone H1.4	5	4.10E-11	−2.54
P16402	H13 Histone H1.3	5	4.10E-11	−2.54
P16403	H12 Histone H1.2	5	4.10E-11	−2.54
P22492	H1T Histone H1t	2	3.60E-05	−7.15
Q02539	H11 Histone H1.1	2	3.60E-05	−7.15
Chaperone				
Q9H1H9	KI13A Kinesin-like protein KIF13A	2	4.20E-02	1.45
Q92688	AN32B Acidic leucine-rich nuclear phosphoprotein 32 family member B	3	5.60E-03	1.33
O75165	DJC13 DnaJ homolog subfamily C member 13	2	2.20E-02	−1.39
P11142	HSP7C Heat shock cognate 71 kDa protein	20	9.90E-20	−1.67
Q15185	TEBP Prostaglandin E synthase 3	3	9.00E-03	−1.89
Protein Biosynthesis and Degradation				
P62195	PRS8 26S protease regulatory subunit 8	2	6.00E-04	2.07
P46778	RL21 60S ribosomal protein L21	2	1.40E-10	1.36
P36952	SPB5 Serpin B5	1	3.90E-02	1.36
P26641	EF1G Elongation factor 1-gamma	10	2.20E-04	−1.36
O00303	EIF3F Eukaryotic translation initiation factor 3 subunit F	2	2.60E-02	−1.37
P58546	MTPN Myotrophin	3	4.20E-03	−1.42
O75153	EIF3X Putative eukaryotic translation initiation factor 3 subunit	2	2.10E-02	−1.43
Q13310	PABP4 Polyadenylate-binding protein 4	3	1.90E-04	−1.48
P62241	RS8 40S ribosomal protein S8	6	6.60E-04	−1.71
RNA processing and Transcriptional Regulation				

Uniprot I.D	Protein	No of Unique Peptides	p-value	Fold Change
Q9UNQ2	DIMT1 Probable dimethyladenosine transferase	2	2.30E-02	2.32
P17096	HMGA1 High mobility group protein HMG-I/HMG-Y	2	9.40E-07	1.68
P42696	RBM34 RNA-binding protein 34	2	3.60E-03	1.56
P17844	DDX5 Probable ATP-dependent RNA helicase DDX5	9	5.90E-03	−1.36
Q9BYG3	MK67I MKI67 FHA domain-interacting nucleolar phosphoprotein	2	4.10E-02	−1.42
Q9NYV4	CD2L7 Cell division cycle 2-related protein kinase 7	5	5.00E-02	−1.44
P84090	ERH Enhancer of rudimentary homolog	2	5.00E-02	−1.99
Kinase activity				
Q15303	ERBB4 Receptor tyrosine-protein kinase erbB-4	2	2.70E-09	1.47
P35590	TIE1 Tyrosine-protein kinase receptor Tie-1	2	1.60E-02	1.36
P30085	KCY UMP-CMP kinase	2	2.80E-02	1.34
Homeostasis				
P20073	ANXA7 Annexin A7	3	4.30E-04	1.46
P08195	4F2 4F2 cell-surface antigen heavy chain	9	1.80E-02	−1.45
P62158	CALM Calmodulin	3	2.50E-02	−1.58
Cell adhesion				
P09382	LEG1 Galectin-1	3	1.20E-05	1.61
Q9Y446	PKP3 Plakophilin-3	3	3.20E-02	−1.39
Apoptosis				
Q13501	SQSTM Sequestosome-1	4	5.80E-05	−1.46
Methylation				
Q6N021	TET2_HUMAN Protein TET2	2	3.10E-03	1.92
O95785	WIZ Protein Wiz	2	3.60E-02	1.47
Centromeric				
Q02224	CENPE Centromeric protein E	2	5.10E-02	2.31
Q9Y6A5	TACC3 Transforming acidic coiled-coil-containing protein 3	2	2.80E-03	1.75
Unknown Function				
Q15847	APM2 Adipose most abundant gene transcript 2 protein	2	1.50E-02	−8.28